Rev. Adv. Mater. Sci. 33 (2013) 281-286

TRIBOLOGICAL BEHAVIORS AND CORROSION RESISTANCE OF ALUMINUM ALLOYS BY NITROGEN PLASMA IMMERSION ION IMPLANTATION

Yehua Jiang[1], Hongxi Liu[1], Rong Zhou[1] and Baoyin Tang[2]

[1]Faculty of Materials Science and Engineering, Kunming University of Science and Technology, Kunming 650093, China
[2]State Key Lab.of Advanced Welding Production Technology, Harbin Institute of Technology, Harbin150001, China

Received: October 17, 2011

Abstract. Nitrogen ions were implanted into LY12CZ aluminum alloy by plasma immersion ion implantation (PIII) technique. The chemical states, composition distributions, tribological properties, and anti-corrosion behaviors of the N-PIII coupons in 3.5% NaCl saturated solution were investigated. X-ray photoelectron spectroscopy (XPS) analysis indicates that the modified layer is mainly composed of AlN phase and a fraction of Al_2O_3 compounds. The depth profile of implanted nitrogen ion has two peaks, corresponding to 40 nm and 88 nm from the surface, respectively. The surface hardness is obviously improved by dispersion strengthening from AlN phase, and the maximum value increases by 140%. Friction and wear behaviors of all these samples exhibits that the friction coefficient reduces from 0.47 to 0.38. Compared with the untreated substrate, the anode polarization curves reveal that the corrosion potential (E_{corr}) of all implanted samples increase and corrosion current density (I_{corr}) decrease, the maximum E_{corr} increases by 200 mV and the minimum I_{corr} decreases by over two orders of magnitude. It also indicates that the wear tracks of modified coupons are much shallower and narrower than that of untreated sample, the minimum wear loss decreases by 43.4%. Tribological property and corrosion resistance of aluminum alloys strongly depended on the composition depth profiles of the modified layers.

1. INTRODUCTION

Aluminum and its alloys are very important metallic structural materials, and widely used in various industrial areas and daily life because of their interesting properties such as light weight, low price, low specific gravity, high strength-to-weight ratio, high electrical conductivity, good machinability and easy production by casting. However, the main limitation of their further widespread applications especially in automotive and space industries is the lack of surface hardness and wear resistance together with low anti-corrosion behavior and chemical stability [1-5].

In order to reinforce aluminum alloy matrix and to improve its wear and corrosion resistance, many kinds of surface modification processes have been developed, such as layer alloying, PVD hard coating, sputter-deposited film, micro-arc discharge oxide coating, plasma-nitrided coating, plasma sprayed coating, plasma immersion ion implantation film and some combination of those methods [6-12]. Among these coating processes, plasma immersion ion implantation (PIII) has been demonstrated to be an attractive and effective approach to enhance the surface properties of aluminum alloy like corrosion and wear resistance and surface hardness [13-15].

Corresponding author: Hongxi Liu, e-mail: piiiliuhx@sina.com

Table 1. Detail experimental parameters of N-PIII.

Sample No.	Implantation ion dose/ (ions·cm^{-2})	Implantation time/ h	Implantation voltage/ kV	Pulse width/ μs	Pulse frequency/ Hz
S1	6.43×10^{16}	1	33	45	200
S2	8.11×10^{16}	1	28	15	300
S3	3.92×10^{16}	1	30	30	100
S4	3.36×10^{17}	3	33	30	300
S5	1.12×10^{17}	3	28	45	100
S6	2.15×10^{17}	3	30	15	200
S7	1.67×10^{17}	5	33	15	100
S8	6.13×10^{17}	5	28	30	200
S9	8.23×10^{17}	5	30	45	300

Particularly, PIII has unique advantages, for example, it has eliminated the line-of-sight restrictions of beam-line implantation, and a cost-effective approach for the surface modification of materials. Therefore, under appropriate conditions, samples with a complicated shape can be treated with good conformity and uniformity without the need to resort to ion beam scanning and special target manipulations. Moreover, one of the features of PIII technique is ability to produce a modified layer with no microscopic defect such as pinholes. In addition, strengthening phase rich in ion implantation modified layer has excellent tribological and anti-corrosion properties. Thus, PIII is the potential modification technique for improving aluminum alloys surface performance [16,17].

In this paper, LY12CZ aluminum alloy was implanted with N by PIII. The chemical state, friction and wear behaviors and corrosion resistance of ion implanted sample surface are studied. The effect of AlN formation on tribological and anti-corrosion performance is also discussed.

2. EXPERIMENTAL PROCEDURES

The substrate material used in this study is commercial aluminum alloy LY12CZ (discs), which contains 4.1 wt.%Cu, 1.4 wt.%Mg, 0.5 wt.%Mn, 0.1 wt.%Ti, 0.2 wt.%Zn, 0.3 wt.%Fe, 0.2 wt.%Si and balance Al. The samples with a size of ∅ 30 mm×4 mm were first solution treatment at 495~503 °C for 30 min, and then aging treatment at 175 °C for 12 h. Prior to vacuum chamber, one side of each coupon was ground with SiC abrasive paper No.400, 800, 1200, and 1500 grits sequentially, followed by polishing with fine diamond paste (average size 0.5 μm) to a roughness of approximately 0.06 mm, and then ultrasonically cleaned with acetone and alcohol for 10 min, respectively. After cleaning ultrasonically, the samples were moved into our multi-purpose PIII facility [18]. The vacuum chamber was evacuated to a base vacuum of 5.0×10^{-3} Pa, and then Ar ion sputtering was introduced into the chamber to remove undesirable oxide and other contamination layers. Nitrogen plasma was produced by radio frequency glow discharge using a pair of filament baskets in a stainless-steel vacuum chamber, 100 cm in diameter and 120 cm in height. The flow rate is 50 sccm, working gas pressure 4.0×10^{-1} Pa. The typical plasma density and electron temperature was measured by a planar Langmuir probe. A water-cooled sample was placed in the center of the chamber (the maximum temperature below 200 °C). Taken into account implantation voltage, implantation time, pulse width and pulse frequency, and design four factors and three level orthogonal experiments, the detail PIII parameters are shown in Table 1.

The surface composition and depth profiles were carried out by X-ray photoelectron spectroscopy (ESCA PHI 5700) by means of argon sputtering using a monochromatic Al K_a radiation. High-resolution XPS spectra were taken at different sputtered depths to investigate the chemical states of the implanted species. The micro-hardness was performed on the HX-1000 micro-hardness tester. The hardness value at every depth was measured for three times, and then an even hardness value was evaluated. A ball-on-disc friction tester was used for the friction tests. During ball-on-disc experiments, the radius of the sliding track was 3 mm; the upper ball was made of silicon carbide (SiC) ceramic, 4 mm in diameter. The rotating velocity was 50 rotations per minute, and the contact load was 0.25 N. The frictional force was transformed by a load cell attached the loading

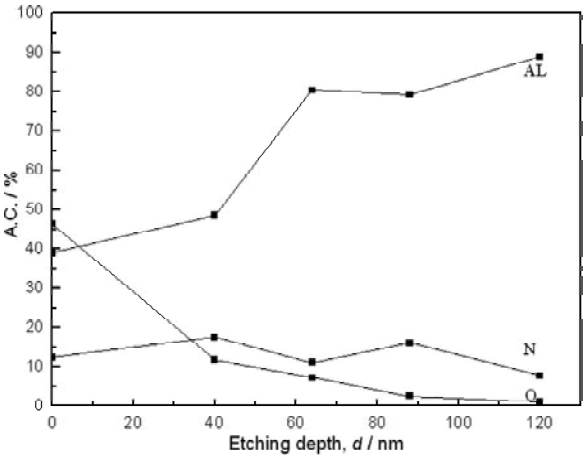

Fig. 1. The concentration depth profile of different elements.

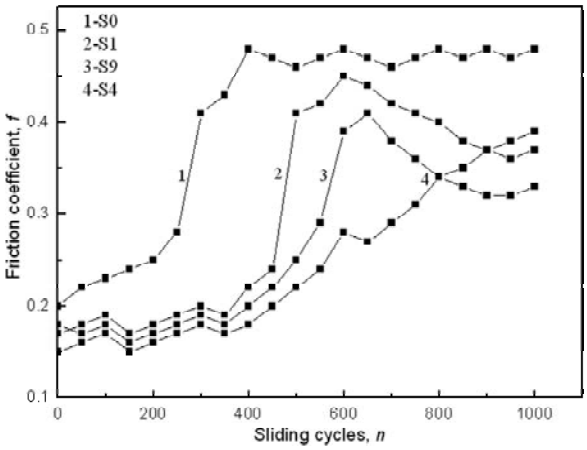

Fig. 2. The relationship of sliding cycles vs. friction coefficient.

arm and recorded by the computer through the data login and requisition system. The depth and the width of the wear tracks were measured with a profilometer, and then the wear volume was obtained. The corrosion and electrochemical behavior of the as-received and N-PIII specimens were determined in 3.5% NaCl aqueous solution using PS-268A electrochemical workstation with a corresponding to computer-driven software. A three-electrode system was employed with the samples as the working electrode, saturated calomel electrode (SCE) as the reference electrode and platinum as the counter electrode. The potential was changed at a rate of 10 mV/s in the range from –1100 to 100 mV. Samples used in the electrochemical test were embedded within epoxy resin and an exposed area of 1.0×1.0 cm^2 was reserved. All the tests were finished under the ambient temperature and the relative humidity was kept 45±5%.

3. RESULTS AND DISCUSSION

The XPS depth profiles of N, O, Al element for sample S6 (4 nm/min calibrated with argon ion gun sputtering) is presented in Fig. 1. It can be seen that the nitrogen depth profile has two peaks (Gaussian-like distribution), corresponding to 40 and 88 nm, with a nitrogen concentration of 17.6 at.% and 15.4 at.%. It is not only different from the LSS calculation of Gaussian distribution, but also different from nitrogen concentration distribution for taking into account the sputtering effect of ion implantation [19]. A considerable amount (peak content approximately 47 at.%) of oxygen in the region near the original sample is retained due to the insufficient sputter time during cleaning with argon ion sputter before ion implantation. The contents of aluminum gradually increase with the increasing in the depth. In addition, there is still contained 7.8% nitrogen in the 120 nm depth. The main reason is that the collision cascade of nitrogen ion implantation process can produce a large amount of interstitial atom and dislocation defects. While the nitrogen atom easy moves along the dislocation line, resulting in the distribution range of nitrogen atoms is wider than that of theoretical calculation data, which is the so-called radiation enhanced diffusion effect.

The binding energy values of nitrogen, aluminum, and oxygen elements in different depth are shown in Table 2. According to XPS database [20], we can see that the binding energy of Al and O in Al_2O_3

Table 2. Binding energy of Nitrogen, Aluminum, and Oxygen at different etching depth.

Etching depth/ nm	Nitrogen binding energy/ eV	Aluminum binding energy/ eV	Oxygen binding energy/ eV
8	399.9	74.7	531.1
40	399.9	74.7	531.1
64	398.5, 396.6	74.7, 74.4, 72.9	531.1
88	398.5, 396.6	74.7, 74.4, 72.9	531.1
120	398.5, 396.6	74.7, 74.4, 72.9	531.1

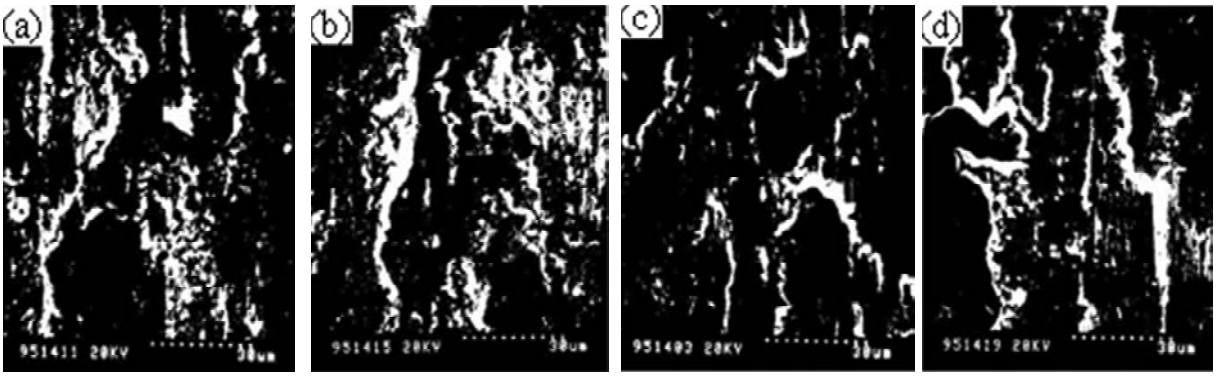

Fig. 3. SEM morphologies of worn tracks on sample S0 (a); sample S1 (b); sample S4 (C); and sample S9 (d) after sliding 600 cycles.

compounds is 74.7 and 531.1 eV; the binding energy of Al and N in AlN compounds is 74.4 and 396.8 eV; and the binding energy of Al and N in a simple substance state is 72.9 and 400.1 eV, respectively. It can be inferred that the presence of aluminum in the surface is Al_2O_3 compounds, and mixture of AlN, Al_2O_3 and simple substance Al in the ion implantation modified layer. The presence of nitrogen is adsorption status in the surface and solution status in ion implantation implanted layer, but the presence of oxygen is Al_2O_3 compounds.

Fig. 2 illustrates the typical curves of friction coefficient of sample S1, S4, S9, and the unmodified sample S0 as a function of sliding cycles. It is apparent that all the friction coefficient curves present a similar pattern, characterized by the initial transient state followed by a first steady state, and then a friction coefficient abrupt increase followed by a gradual-steady state. The initial transient state corresponds to the contact of the highest asperities of the disk and ceramic ball surfaces. The first steady state indicates the real contact of the two surfaces, corresponding to the friction coefficient between the modified layer and the ceramic ball. The friction coefficient abrupt increase means the ion implantation modified layer is just worn out, corresponding to the wear life. The gradual-steady state implies the contact between the ceramic ball and first part of the substrate, and then gradually the whole substrate. It can be noted that the friction coefficient of treated samples is lower than that of bare aluminum alloy at the beginning (about less than 300 sliding cycles). This is because there is a large amount of small size, dispersed AlN hard phase in the modified layer; it can increase the surface hardness and decrease the friction coefficient. During the sliding cycles of 300 to 600, the friction coefficient of N-PIII samples increase slowly, but still lower than that of the virgin sample. The main reason is that the implanted layer has been worn out, but nitrogen atoms can diffuse along the high density dislocation direction and strengthen the matrix. When the sliding cycles exceeds 600 cycles, the friction coefficient of all samples displays the same trend. This is because the surface layer is worn out and ceramic ball contacts the aluminum alloy substrate. According the friction curves, the aluminum alloy substrate has the shortest wear life (approximately 400 cycles) and the highest friction coefficient (about 0.47), and the modified layer of sample S4 has the longest wear life (over 1000 cycles) and lowest friction coefficient (about 0.38). It is clear that the friction coefficient and the wear life of N-PIII aluminum alloy have been improved obviously.

Fig. 3 shows the SEM micrographs of the wear tracks of sample S1, S4, S9, and substrate S0 worn for 600 cycles under the same conditions. As shown in Fig. 3a, the wear tracks of substrate present the adhesive wear mechanism, and on which there are obvious pits and big pieces of transferred substances. The transferred substances are proved to be Al and a small amount of ceramic ball. This implies that its surface layer has been worn out. However, under the same conditions, the wear tracks of S1, S4, and S9 are not obvious, only with smooth and mild scrapes and some little fine transferred substances containing Al as exhibited in Figs. 3b, 3c, and 3d. This indicates that its modified layer has not been worn out, with some transferred substances from the ceramic ball. In addition, the wear track of S4 is still shallower and narrower than those of sample S1 and S9, the adhesive degree reduces significantly. This proofs that the wear resistance of S4 has been improved much more than that of S1 and S9. The superior wear resistance of sample S4 can be attributed to its high hardness,

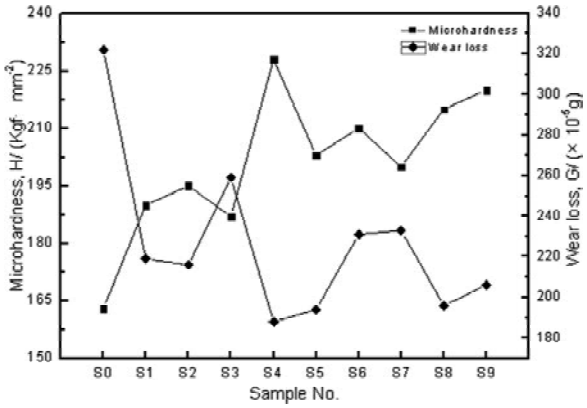

Fig. 4. The microhardness and wear weight loss of different samples.

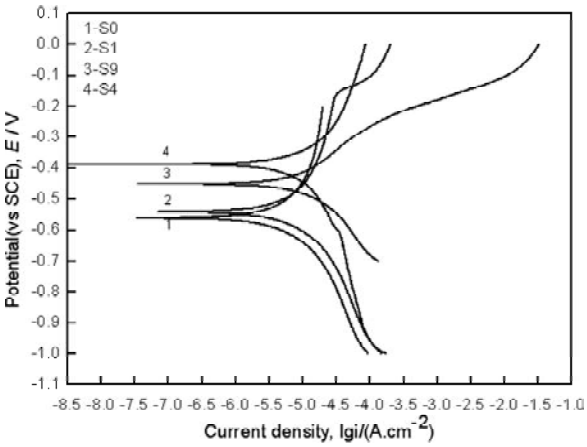

Fig. 5. The polarization curves of untreated sample S0 and treated samples S1, S4, and S9.

low friction and ion implantation modified layer in the substrate.

The Vickers micro-hardness (HV0.025) and wear loss test results of the samples before and after N-PIII are shown in Fig. 4. It is evident that the micro-hardness of the PIII samples is higher than that of untreated sample (163 HV0.025); and the micro-hardness changes in good agreement with the sliding wear behavior of the PIII-treated aluminum alloy as shown in Fig. 2. Under the same loading, the sample S4 shows the highest micro-hardness of 228 HV0.025, increase by 140%. This is because the near surface layers consist of a mixture of hard Al_2O_3 and AlN phases, which give a higher hardness value. In addition, the effect of nitrogen solid solution strengthening in the aluminum alloy substrate also plays an important role in improving the surface micro-hardness of treated samples. In addition, under the same condition, the cumulative wear weight loss of aluminum alloy substrate is 3.22 mg, but wear loss of sample S4 is 1.88 mg, decreases by 43.4%.

The polarization curves of treated and untreated samples in 3.5% NaCl saturated solution are exhibited in Fig. 5. It can be seen that nitrogen plasma immersion ion implantation significantly reduced the corrosion current density of the aluminum alloy and shifted the corrosion potential to a more positive value, depending on the nitrogen ion implantation dose. Compared with the substrate, corrosion potentials E_{corr} changed from -580 mV of the bare sample S0 to -380 mV of sample S4 with a maximum increment of 200 mV. Corrosion current density I_{corr} of N-PIII coupons declined strongly over one or two orders of magnitude. From a thermodynamical point of view, the more corrosion resistance shifts positive, the harder corrosion phenomena of the sample occur. The better corrosion performance of the N-PIII aluminum alloy was attributed to beneficial hardening phase aluminum nitride in the modified layer and oxide aluminum in the surface layer. Therefore, N-PIII can effectively enhance corrosion resistance of LY12CZ aluminum alloy.

4. CONCLUSION

Nitrogen ions were implanted into LY12CZ aluminum alloy by plasma immersion ion implantation technique. The XPS analysis indicated that the nitrogen depth profile had two peaks (Gaussian-like distribution), corresponding to 40 and 88 nm from the outer surface, and the maximum depth of the implanted layer is approximately 120 nm. The XPS results also confirmed the formation of AlN phase and Al_2O_3 compounds in the near surface region. The micro-hardness of N-PIII sample is increased by 140%, the friction coefficient reduced from 0.47 to 0.38, and the wear loss decreased by 43.4% in contrast with those of the untreated sample. The corrosion potential shifted to positive 200 mV and the corrosion current density declined over one or two orders of magnitude, depending on the nitrogen ion implantation dose. The dispersion of AlN precipitates and supersaturated solid solution of nitrogen in the modified layer was the main strengthening mechanism to improve the tribological properties and corrosion resistance of LY12CZ aluminum alloy.

ACKNOWLEDGEMENTS

This research was jointly supported financially by the National Nature Science Foundation of China (Grant No.50671045), the Nature Science Foundation of Yunnan Province (Grant No.

2008ZC021M) and the analysis and testing foundation of Kunming University of Science and Technology (2009-022). The authors wish to express their gratitude to Dr. J. H. Lu, who performed the XPS analyses. The authors also would like to thank Dr. C.J. Zhang for his help in the SEM observation.

REFERENCES

[1] K. Baba, R. Hatada, S. Flege, G. Kraft and W. Ensinger // *Surf. Coat. Technol*. **203** (2009) 2617.
[2] N. Arun Prakash, R. Gnanamoorthy and M. Kamaraj // *Mater. Sci. Eng. B* **168** (2010) 176.
[3] P. Budzynski, A.A. Youssef, Z. Surowiec and R. Paluch // *Vacuum* **81** (2007) 1154.
[4] Halil Demir and Süleyman Gündüz // *Mater. Design* **30** (2009) 1480.
[5] Ming Xu, Xun Cai, Youming Liu, Shihao Pu and Paul K. Chu // *Dia. Relat. Mater.* **17** (2008) 1844.
[6] Ouming Liu, Liuhe Li, Ming Xu, Xun Cai, Qiulong Chen and Paul K. Chu // *Mater. Sci. Eng. A* **415** (2006) 140.
[7] H.R. Zhou, X.G. Li, J. Ma, C.F. Dong and Y.Z. Huang // *Mater. Sci. Eng. B* **162** (2009) 1.
[8] Yang Li and Liang Wang // *Thin Solid Films* **517** (2009) 3208.
[9] P.Eh. Hovsepian, Q. Luo, G. Robinson, M. Pittman, M. Howarth, D. Doerwald, R. Tietema, W.M. Sim, A. Deeming and T. Zeus // *Surf. Coat. Technol.* **201** (2006) 265.
[10] Beril Çorlu and Mustafa Ürgen // *Surf. Coat. Technol.* **204** (2009) 872.
[11] Qizheng Li, Yuming Tang and Yu Zuo // *Mater. Chem. Phys.* **120** (2010) 676.
[12] Ghulam Murtaza, S.S. Hussain, Mehboob Sadiq and M. Zakaullah // *Thin Solid Films* **517** (2009) 6777.
[13] J.X. Liao, L.F. Xia, M.R. Sun, Y. Sun, W.M. Liu, T. Xu and Q.J. Xue // *Wear* **256** (2004) 840.
[14] Ibrahim Etem Saklakoğlu // *J Mater. Process. Tech.* **209** (2009) 1796.
[15] K. Baba, R. Hatada, S. Flege, G. Kraft and W. Ensinger // *Surf. Coat. Technol.* **203** (2009) 2617.
[16] M.I. Current, W. Liu, A.J. Lamm, L. Feng, S. Qin, C. Chan and N.W. Cheung // *Surf. Coat. Technol.* **136** (2001) 138.
[17] P.K. Chu, S. Qin, C. Chan, N.W. Cheung and L. A. Larson // *Mater. Sci. Eng. R* **17** (1996) 207.
[18] S.Y. Wang, P.K. Chu, B.Y. Tang and X.C. Zeng // *Nucl. Instru. Meth. Phys. Res. B* **127-128** (1997) 1000.
[19] K. Yukimur // *Surf. Coat. Technol.* **136** (2001) 1.
[20] J. F. Moulder and F. S. William, *Hangbook of X-ray Photoelectron Spectroscopy* (Physics Electronics Inc., 1991).